Multiscale effects in sodium fast reactors : feedback from the open phase of the FFTF LOFWOS-13 test

Antoine Gerschenfeld, Yannick Gorsse, Simon Li

Multiscale Effects in Sodium Fast Reactors : Feedback from the Open Phase of the FFTF LOFWOS-13 Test

Antoine Gerschenfeld[1], **Yannick Gorsse**[1], **and Simon Li**[2]
[1]Université Paris-Saclay, CEA, Service de Thermo-hydraulique et de Mécanique des Fluides, Gif-sur-Yvette, France
[2]CEA Cadarache, 13115 Saint-Paul-lez-Durance, France
antoine.gerschenfeld@cea.fr; yannick.gorsse@cea.fr; simon.li@cea.fr

ABSTRACT

Sodium and lead-cooled liquid-metal reactors often feature large liquid-metal pools, where complex 3D phenomena may take place during loss-of-flow or loss-of-heatsink transients. This concern has given rise to the development of new modelling approaches aimed at integrating the result of subchannel and/or CFD models into an overall reactor calculation: these "multi-scale" simulations have been applied, among others, to the PHENIX natural convection [1] and dissymmetric [2] tests and to the EBR-II loss-of flow tests [3], as well as to several liquid-metal experiments.

In the context of a recently-concluded IAEA CRP [4], the FFTF "LOFWOS-13" unprotected loss-of-flow test has been analyzed at CEA with the MATHYS multi-scale coupling code [5]: on the basis of simulations performed at imposed power, this paper details the influence of 3D phenomena in the primary vessel on the overall transient. Because of the loop-type design of the reactor, these phenomena have little to no influence on the primary flowrate and inlet/outlet temperatures: however, in-vessel measurements, and in particular subassembly outlet temperatures, are strongly affected by the 3D behavior of the temperature field at the core outlet and its propagation above the core.

Consequently, the multiscale simulation is not indispensable to the system-scale analysis of the overall transient: however, it can play an important role as a "numerical twin" to the experimental data, helping to understand how local measurements may differ from the averages predicted by a system-scale approach. The possible effect of 3D phenomena outside the vessel, such as stratification in the piping, will be analyzed in future work.

KEYWORDS
numerical scheme, subchannel, multiphase, SFR, sodium boiling

1. INTRODUCTION

Past safety assessments of Sodium Fast Reactor (SFR) designs, such as PHENIX and SUPERPHENIX in France, have relied on System Thermal-Hydraulics (STH) analysis for the prediction of thermal-hydraulic transients such as Loss Of Flow (LOF) and Loss Of Heatsink (LOHS) accidents. Pioneered for loop-type pressurized-water reactors, STH relies on a 0D-1D nodalization of one or more reactor circuits, coupled to thermal structure models for the core and heat exchangers and, in the case of unprotected transients, to a point-kinetics model of the core neutronics: more recently, coarse 3D nodalizations have been introduced in system codes such as RELAP5 [6], CATHARE [7] and TRACE [8] to model phenomena such as flow distribution and mixing in the downcomer, core and inlet/outlet plena of PWRs.

SFRs, and more generally liquid-metal reactors (LMR), often feature large liquid metal pools at the outlet of the core and/or primary heat exchangers as a result of adopting a pool-type primary circuit configuration:

even in loop-type designs, the need to perform under-sodium fuel handling results in the presence of a large sodium plenum above the core. Liquid flows in these plena will be convection-dominated in normal operation, but buoyancy-dominated in low-flow accidental conditions: additionally, dissymetric transients (such as the loss of a single pump or intermediate loop) often lead to complex mixing effects. Additionally, large LM pools allow for passive decay heat removal by placing dipped heat exchangers in the hot pool or by cooling the reactor vessel from the outside : these systems, known respectively as DRACS and RVACS [9], also lead to complex flow patterns in the primary circuit, and in particular to natural convection loops in the inter-wrapper region separating the core subassemblies [10].

The 3D phenomena outlined above are only partly accessible to the coarse 3D nodalizations available in STH codes: while stratification in a pool can be modelled with reasonable accuracy using a coarse mesh [11], the behavior of an incoming jet and its interaction with such a stratification requires a finer mesh (on the order of a few million cells) [2]. Predicting the effect of inter-wrapper flow of core cooling is similarly difficult, requiring an explicit mesh for the inter-wrapper region as well as a thermal-hydraulic model inside each S/A capable of predicting its internal temperature distribution. This need has motivated the development of a number of new approaches, based on either simulating the complete primary circuit at the CFD scale, or on integrating a CFD simulation of a region of interest with a global STH model. At CEA, the simulation needs of the ASTRID program led to the development of the multi-scale coupling code MATHYS [5], in which:

- the complete primary circuit, as well as other circuits (intermediate or DHR loops, power conversion system) are simulated by the CATHARE STH code;
- regions affected by 3D phenomena such as the core, large plena and intermediate heat exchanger (IHX) primary sides are simulated by the subchannel code TrioMC [12] and the CFD code TrioCFD [13]. Results from these simulations are fed back to the corresponding regions in CATHARE by a process known as “domain overlapping”, ensuring that the three codes perform a consistent simulation of the complete reactor transient.

The choice of multiscale coupling over a “full-CFD” approach maximizes the reuse of existing models in each code and their associated “separate effect” validation: on the other hand, coupled effects, such as the core-pool interaction during hot-pool DRACS, can not be predicted by a single code and must thus be validated by a new Integral Effect Test (IET) database. These IET should ideally be complemented by as many integral tests as possible. The MATHYS validation database currently includes three IETs (THEADES [14] for core-IWF coupling, TALL-3D [15] for loop-pool coupling, and PLANDTL-1/2 [10, 16] for core-pool coupling) and two integral tests (the PHENIX end-of-life natural convection [1] and dissymetric [2] tests).

In 2019, DOE offered a new opportunity for SFR integral validation by sponsoring an IAEA CRP [4] on the FFTF reactor. Operated from 1980 to 1992, FFTF was a 400MWth, loop-type SFR dedicated to the qualification of fuel and components of the US SFR program: in 1986, it was subjected in a number of passive safety tests [17], culminating with an unprotected loss flow from 50% initial power known as LOFWOS#13 (Loss Of Flow WithOut Scram). As part of its participation in the IAEA CRP, CEA developed CATHARE and MATHYS models of FFTF: results from the latter were submitted to DOE and IAEA in the initial (blind) and final (open) parts of the benchmark. In this last part, measured core power was transmitted to the CRP participants so that they could improve their simulations.

Taking advantage from the availability of the transient power history, this paper aims to assess the relevancy of 3D phenomena during the LOFWOS#13 transient by comparing CATHARE and MATHYS simulations of the transient at imposed power to the experimental data. This analysis leads to the following conclusions:

- the overall behavior of the transient, such as the flow-rate decrease and transition to natural convection and core inlet temperature, are not affected by 3D phenomena;
- some global parameters, such as the primary vessel outlet temperature, show a moderate effect;
- finally, local measurements, such as thermocouples located at the core outlet, show a strong effect.

Hence, the overall behavior of FFTF during the LOFWOS#13 transient can be correctly predicted by the system scale: on the other hand, local measurement are hard to reproduce without a more complex multiscale and/or CFD model. These approaches can thus play a role as a "numerical twin" of the reactor, giving insights into how local measurements should be interpreted in comparison to the average results provided by STH: trying to "improve" the STH results to improve the calculation-experiment difference for these measurements would indeed be improductive and degrade the overall accuracy of the STH simulation.

The paper is organized as follows:

- the FFTF reactor and the LOFWOS#13 test are presented in Section 2;
- the CATHARE and MATHYS models of FFTF are described in Section 3;
- Global results of both simulations are compared to the experiment in Section 4;
- Local results in both simulations are compared to the experiment in Section 5.

2. THE FFTF REACTOR AND LOFWOS#13 TRANSIENT

Constructed from 1970 to 1978 at Hanford, the Fast Flux Test Facility (FFTF) was operated from 1981 to 1992 with the primary goal of qualifying fuel and components for the US fast reactor program and in particular the Clinch River Breeder Reactor (CRBR) project. FFTF, like CRBR, is a loop-type reactor: the 400MW nominal power is transported from the primary vessel (fig. 1, left) by three primary loops (fig. 1, top right) to tube-shell intermediate heat exchangers (IHX). Three secondary loops (fig. 1, bottom right) connect the tube side of these IHXs to sodium-air dump heat exchangers (DHX). The reactor core consists in 199 hexagonal subassemblies: among those, the 74 fuel assemblies contain a 217-pin, wire-spaced pin bundle of mixed uranium-plutonium oxide fuel.

Like EBR-II, FFTF underwent in 1986 a series of Passive Safety Tests [17]. These tests included static neutronic tests, natural-convection thermal hydraulic tests, and finally a series of Unprotected Loss-Of-Flow (ULOF) tests at increasing initial power. Unlike metal-fueled SFRs, oxide-fuel SFRs operate with a large average fuel temperature: during an ULOF, this temperature decreases rapidly, leading to a large positive Doppler reactivity feedback. During its ULOF tests, known as LOFWOS, FFTF was equipped with a number of Gas Expansion Modules (GEMs) [18]: these innovative devices had the effect of increasing lateral neutron leakage at low flowrate, countering the positive fuel Doppler reactivity and ensuring that the reactor would reach a natural-convection, low-power final state without reaching high sodium temperatures.

The highest-power LOFWOS test, LOFWOS#13 starting from 50% initial power, was provided by DOE to IAEA in the framework of a Collaborative Research Program (CRP) in 2018. The following measurements are available over the 900-second transient;

- in the core, the neutronic power history and initial total power were measured, as well as the core outlet temperatures at two subassembly positions (PIOTA2 at the center and PIOTA6 at the periphery);
- flowrate, inlet/outlet temperature and pump speed in each of the 3 primary loops;

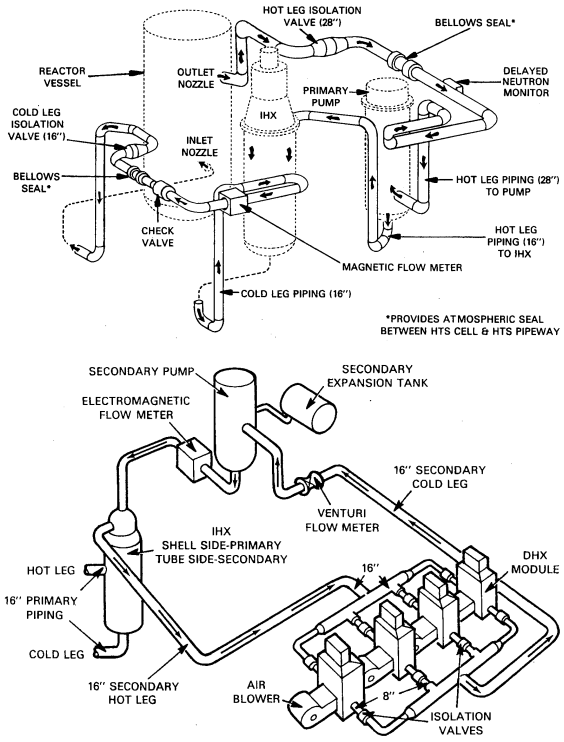

Figure 1. Design of the FFTF reactor [19]: primary vessel (left), primary loop (top right), secondary loop (bottom right).

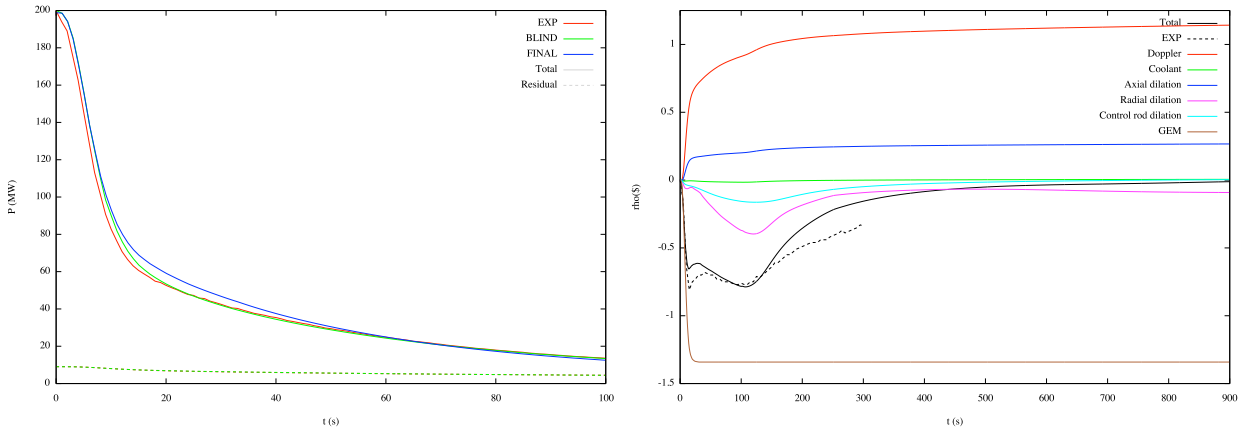

Figure 2. Power and reactivity in the LOFWOS#13 test: experimental power and prediction in the blind/final CEA calculation (left), reactivity decompostion in the final CEA calculation (right). In the calculations presented in Sections 4 and 5, the measured power (left, in red) is a boundary condition.

- flowrate, inlet/outlet temperature and pump speed in each of the 3 secondary loops as well as the average DHX outlet temperature.

In an initial "blind" phase, the 25 CRP participants simulated the transient using the initial state of the reactor, the primary/secondary pump speeds and the DHX outlet temperatures as boundary conditions: in a subsequent "open" phase, all measurement were made available so that participants could further improve

their models.

Figure 2 shows the calculation-experiment comparison for the CEA CRP calculations for power (left) and reactivity (right). Aside from the GEM reactivity effect (show in brown), many reactivity contributions introduce large uncertainties: these include the core radial expansion (affected by a core restraint system), its axial expansion (potentially affected by pin-cladding interaction), control rod driveline expansion and Doppler effect (affected by fuel thermal conductivity and gap conductance). These effects can make it difficult to isolate the impact of thermal-hydraulic phenomena when analyzing calculation-to-experiment discrepancies. Thus, additional simulations using the experimental neutronic power history as a boundary condition were performed for the purpose of this paper: this allowed us to concentrate on those model-to-experiment discrepancies resulting only from thermal-hydraulic effects.

3. CATHARE AND MATHYS MODELS OF THE FFTF

As a participant in the FFTF CRP, CEA developed two models of the reactor: a CATHARE model of the primary and secondary circuits and a MATHYS model coupling this model to a subchannel/CFD model of the primary vessel, consisting in a TrioMC subchannel model of the core and a TrioCFD CFD model of the rest of the primary vessel.

The CATHARE model (fig. 3) relies on a multi-channel model of the core (fig. 3a), in which the 199 core subassemblies are grouped into 16 channels. In the 7 channels corresponding to the fuel S/As, thermal structures model the fuel itself: in the model used in the CRP calculations, the calculated fuel temperature is used in a point-kinetics neutronic model to predict the reactor power. Outside the core, the inlet and outlet plena in the primary vessel are described by 0D volumes (fig. 3b). Notable correlations used in the core include the Rehme bundle pressure drop correlation [20] and the Skupinski heat transfer correlation [21]. Because the three FFTF primary loops exhibit slightly different behavior both in steady-state and during the transient, the CATHARE model describes each primary and secondary loop separately. Each primary loop includes :

- a 1D hot leg, in which the “primary hot leg” thermocouple is located;
- a primary pump described by its octants and following the experimentally measured pump speed;
- a shell-side IHX primary side, where heat transfer is modelled by the Borishanski correlation [22];
- and a 1D cold leg, where the “primary cold leg” thermocouple is located.

Contrary to the primary loops, the secondary loops are only described partially:

- the secondary cold leg is described from the “secondary cold leg” thermocouple location, where the experimental temperature and flowrate in each loop are imposed as boundary condition;
- the central tube and the shell side of each IHX, with heat transfer described by the Skupinski correlation;
- the secondary hot leg is only described up to the “secondary hot leg” thermocouple location.

The MATHYS model couples CATHARE to a subchannel/CFD model of the primary pool (fig. 4), in which:

- the core and inter-wrapper region are described at the subchannel scale using the TrioMC subchannel code, using 2.9M meshes. Notable correlations used include the Pacio-Cheng-Todreas axial pressure drop corrleation [23], the Cheng-Todreas wire mixing correlation [24], the Gunther-Shaw transverse

pressure drop correlation [25], and the Seban-Shimazaki heat transfer correlation [26]. The FFTF core includes large "load pads" at two levels (top of fissile zone and core outlet), where the subassemblies are almost in contact. In the TrioMC model, it was assumed that inter-wrapper flow is completely blocked at these levels. Above the core, the bottom part of the upper instrument shield (UIS) is modelled: this includes the two core outlet thermocouple locations.

- The surrouding vessel, consisting in inlet and outlet plena as well as a vessel cooling system, are modelled at the CFD scale using the TrioCFD code with 5.4M fluid meshes. Because of the large thermal conductivity of liquid sodium, the effect of turbulence on heat transfer is ignored. The core is surrounded radially by a large "radial shield": this structure is represented by a monolithic steel structure.

The TrioMC and TrioCFD portions of the model are solved simultaneously thanks to the use of a common numerical scheme ("PolyMAC") [27]: at each time step, each step of the solution (velocity prediction, pressure resolution, temperature prediction) is performed using a single linear system. MATHYS performs a looser coupling between this subchannel/CFD pool model and the overall CATHARE model [5]. At each time step:

- the subchannel/CFD model uses the primary loop flowrates and temperatures computed by CATHARE as inlet boundary conditions;
- the average temperatures observed in the subchannel/CFD model at the primary outlets are imposed

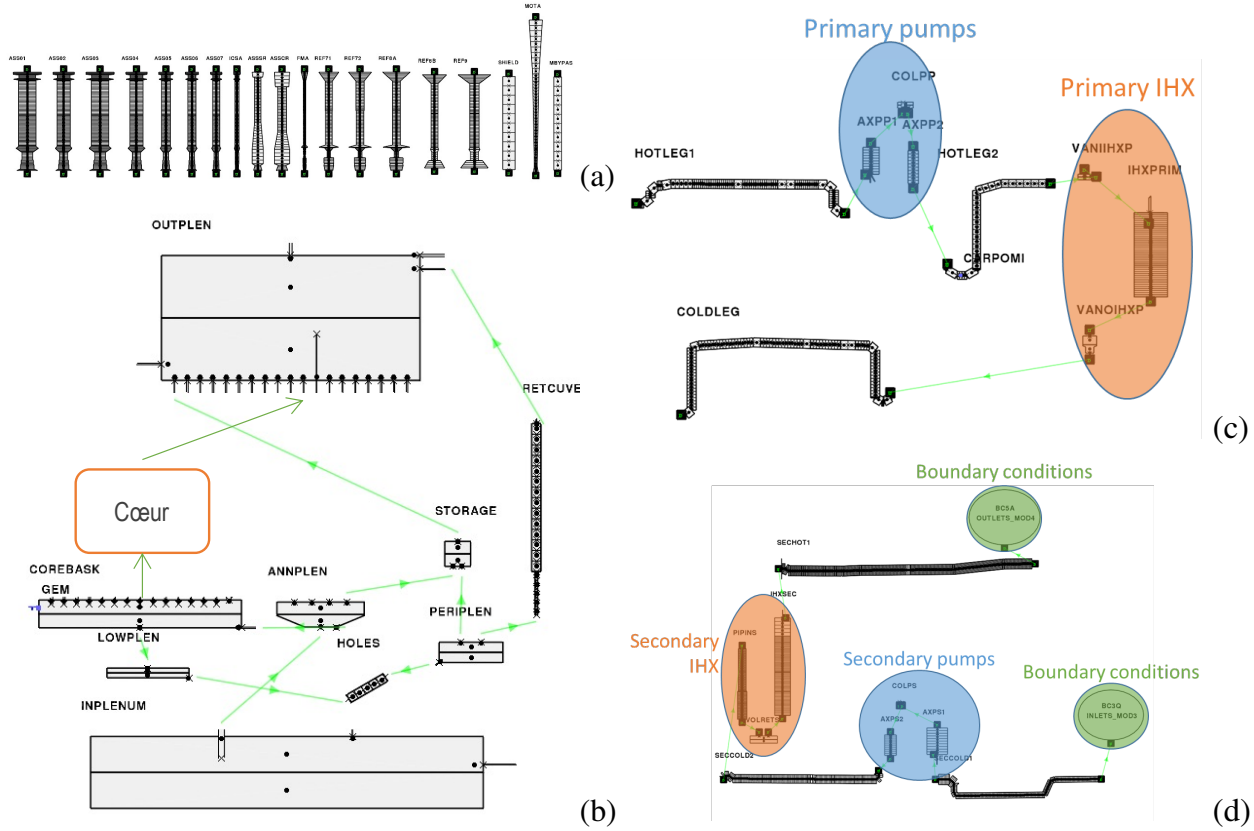

Figure 3. CATHARE model of FFTF: core channels (a), primary vessel (b), primary loop (c), secondary loop (d).

in the corresponding CATHARE locations;

- momentum source terms F_{ij} are imposed in CATHARE so that the pressure differences Δp_{ij} between any two inlet/outlets are the same in CATHARE as in TrioMC/CFD. The correct values of the F_{ij} are obtained by performing internal iterations at each time step: in most cases, this only results in an additional CATHARE iteration compared to a non-coupled calculation.

This coupling algorithm ensures that, at each time step, the CATHARE and TrioMC/CFD simulations are consistent in terms of pressure drops, flowrates and temperatures. Its numerical cost is somewhat low in practice, entailing no extra CFD iterations and one extra STH iteration compared to the non-coupled case. The CATHARE model used in MATHYS is the same as those used in the standalone CATHARE simulations: thus, the results of the two models can be compared directly to analyze the effect of 3D phenomena.

The two simulations exhibit very different numerical requirements:

- the CATHARE simulation can be performed in around 10 minutes on one core (Apple M1, 3.2 GHz);
- the MATHYS simulation takes around 8 hours on 1024 cores (AMD EPYC 7281, 2.4 GHz).

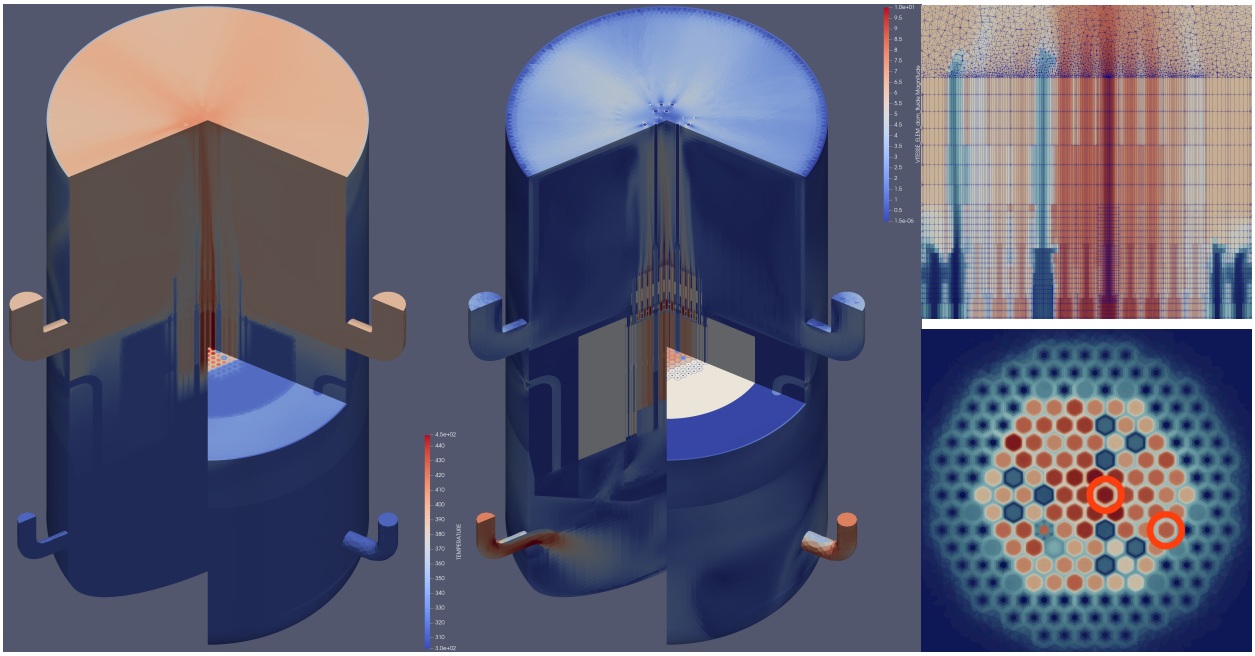

Figure 4. TrioMC/TrioCFD model of the FFTF primary pool: initial temperature field (left) and velocity field (center), vertical (top right) and radial (bottom right) temperature field at core outlet.

4. IMPACT OF 3D PHENOMENA ON THE GLOBAL REACTOR BEHAVIOR

Given that the CATHARE and MATHYS calculations for this article were performed at imposed power, global transient parameters of interest are the hot/cold temperatures and flowrate in each loop: this last parameter is only of interest in the primary loops, given that the secondary loop were kept in forced convection over the duration of the transient.

The primary flowrate in each loop is shown in fig. 5. The short-term flow decrease (left) and the long-term natural convection flowrate (right) are predicted well by both CATHARE and MATHYS, with little differ-

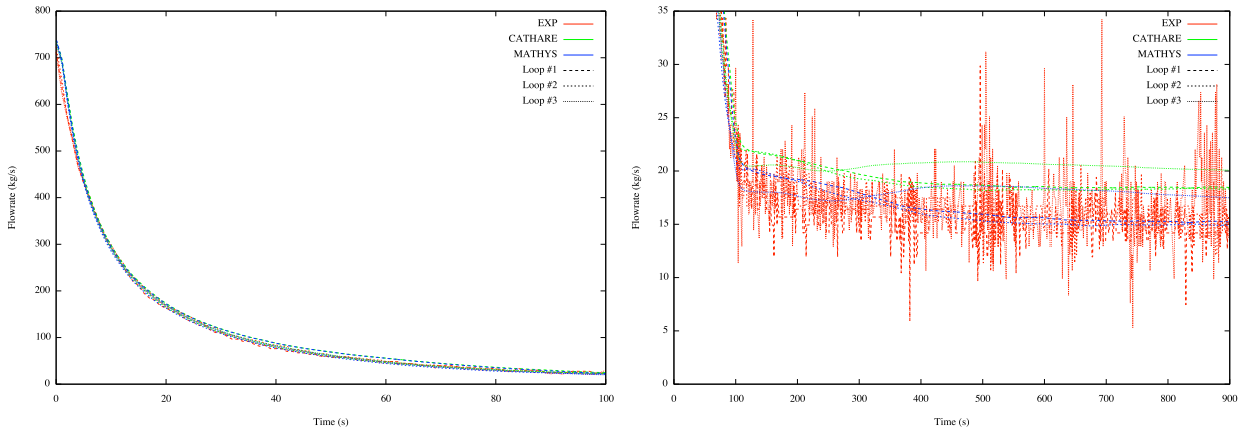

Figure 5. Short-term (left) and long-term (right) primary flowrate during LOFWOS#13: experimental results (red), CATHARE (green) and MATHYS (blue) calculations for each primary loop.

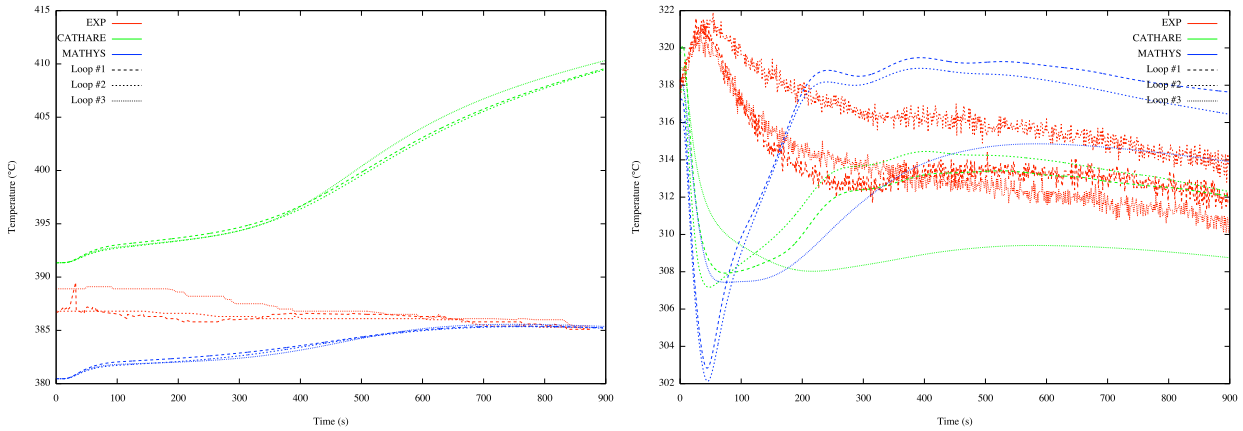

Figure 6. Hot leg(left) and cold leg(right) primary temperatures during LOFWOS#13: experimental results (red), CATHARE (green) and MATHYS (blue) calculations for each primary loop.

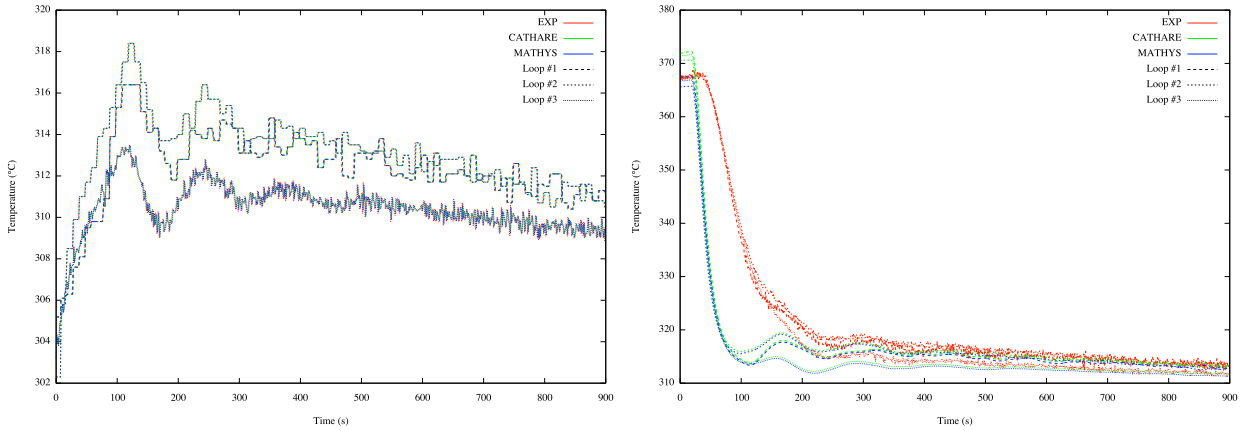

Figure 7. Cold leg(left) and hot leg(right) secondary temperatures during LOFWOS#13: experimental results (red), CATHARE (green) and MATHYS (blue) calculations for each primary loop.

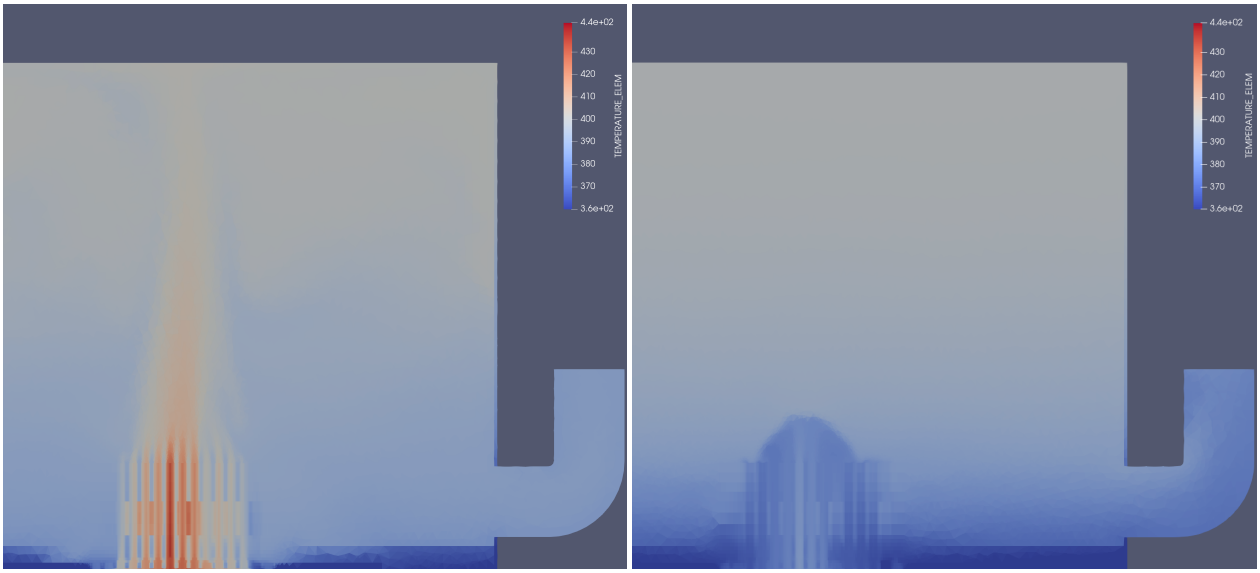

Figure 8. Upper plenum stratification in the MATHYS calculation: temperature field from the core outlet to the hot legs at $t = 250$s (left) and $t = 750$s (right).

ence between the two simulations. The high precision of both predictions results from the good accuracy of the primary loop temperatures, shown in Figure 6: since the cold and hot leg temperature predictions are quite close to the experimental results (by 5-10°), and given the loop-type nature of FFTF, it is not surprising that the natural convection flowrate is predicted well.

Taking a closer look at the primary loop temperatures (fig. 6), MATHYS and CATHARE predict significantly different trends in the hot legs (left), with CATHARE showing a 20° temperature increase over the course of the transient while MATHYS predicts a flat trend more consistent with the experimental results. This is because the CATHARE model assumes perfect mixing in the outlet plenum (which it models as a 0D volume). Meanwhile, in the MATHYS calculation, TrioCFD predicts a thermal stratification (fig. 8):

- as the core outlet temperature rises (fig. 8, left), the outlet jet ascends to the top of the outlet plenum, while the bottom of this plenum (where the hot leg intakes are located) remains at a cooler and somewhat constant temperature;
- later in the transient (fig.8, right), the core outlet jet cools down and flows directly into the hot legs through the bottom of the plenum, while the hotter sodium above remains stagnant.

The consistency of the experimental data with the MATHYS results seems to indicate that this phenomenon does occur during LOFWOS#13. However, this has little to no impact on the primary cold leg temperatures shown in Figure 6 (right), where the CATHARE and MATHYS predictions are very close. This is caused by the transient conditions: because the secondary loops are kept in forced convection, the IHXes act as an "imposed temperature" heat sink, and tend to cool down the primary sodium to the secondary cold leg temperature of 310-312° very efficiently. As a consequence, the primary cold leg temperatures predicted by CATHARE and MATHYS are almost identical to the experimental value, resulting in very close natural convection flowrates.

Closer analysis reveals that CATHARE and MATHYS both predict a ~ 10°C initial cold shock in the cold legs, unlike the experimental data: similarly, while the secondary cold leg temperature (fig. 7, left) and

flowrates are imposed from experimental boundary conditions, the secondary hot leg temperatures (fig. 7, right) decrease much faster in CATHARE and MATHYS than in the experiment. The experimental delay in the secondary cold leg temperature drop could be caused by an underestimation of the IHX thermal inertia: on the other hand, the initial hot shock in the primary cold leg seems harder to explain. In pool-type reactors, decreases in the primary flow typically lead to a change in the IHX outlet jet and thereafter to a different downstream temperature: possibly, this phenomenon could take place at a smaller scale in the FFTF IHXes and produce a small hot shock. In order to confirm this, it would be necessary to include a 3D model of the IHX primary sides in the MATHYS simulation.

Figures 5-7 thus show that 3D phenomena only have a weak effect on the overall transient parameters, and almost no effect on the primary flowrate: this is caused both by the loop-type configuration of the primary circuit and by the transient conditions, in which forced convection in the secondary circuit dampens the impact of local effects on the overall behavior.

5. IMPACT OF 3D PHENOMENA ON LOCAL MEASUREMENTS

In addition to the global power, temperature and flowrate measurements described in Section 4, two local measurements were provided by DOE as part of the LOFWOS#13 data package: temperature measurements at the outlet of two subassemblies, PIOTA2 at the center of the core and PIOTA6 at the core periphery. The radial positions of these two measurements in the core, as well as details of the thermocouple probes used, are shown on Figure 9. One can readily notice that:

- the PIOTA probes are inserted in an adapter that almost completely covers the underlying subassembly outlet, so that each PIOTA probe is insulated from sodium coming out of the neighbouring S/As. Thus, PIOTA measurements are not affected by mixing and deviation effects at the core outlet;
- each PIOTA probe measurements is the average of three temperature measurements placed around the probe center. Hence, if a radial gradient is present in the subassembly outlet jet, then the probe measures neither the average nor the maximum temperature in this jet, but rather an intermediate value.

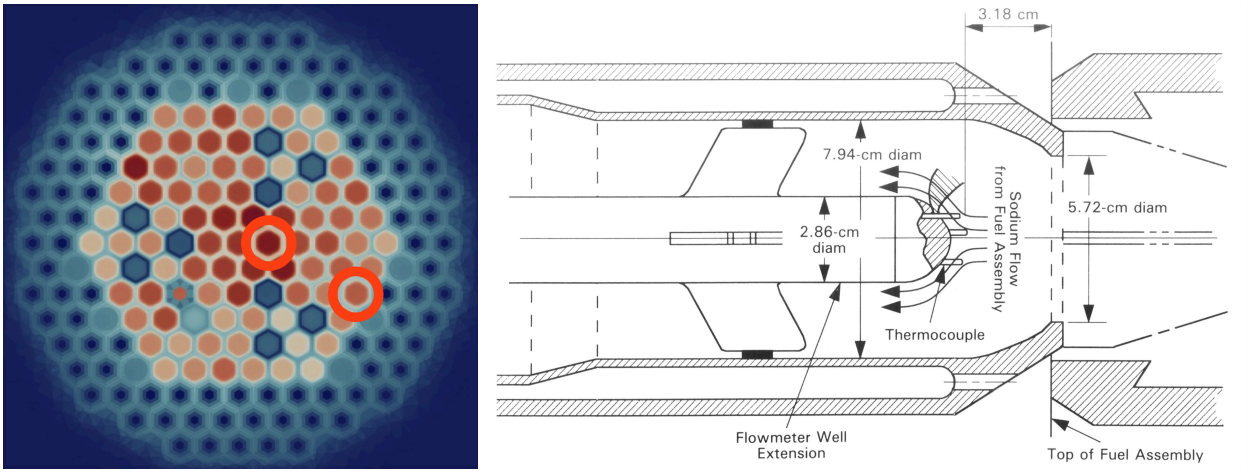

Figure 9. Location of the PIOTA2 and PIOTA6 core outlet temperature measurements during the LOFWOS#13 transient: radial position (left), thermocouple probe detail [17] (right).

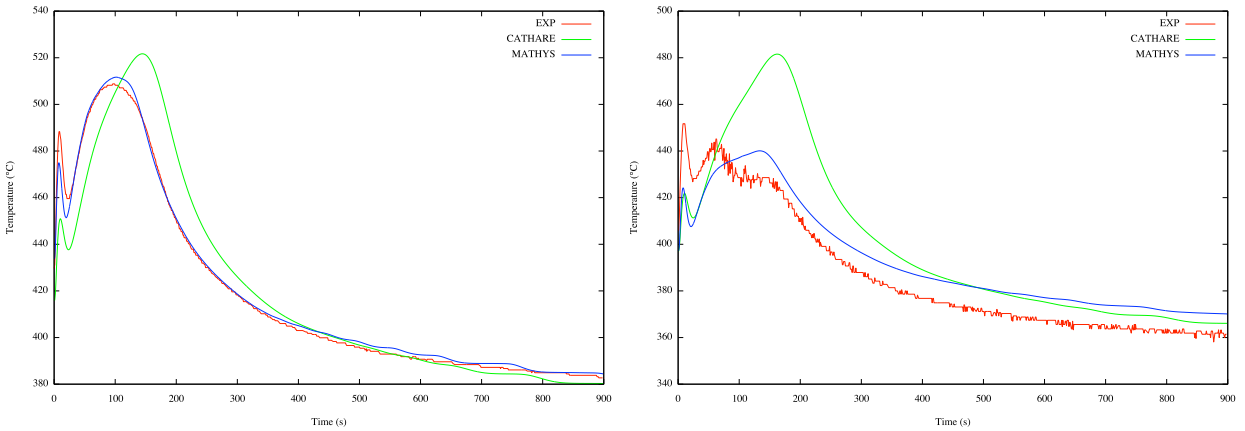

Figure 10. PIOTA2 and PIOTA6 core outlet temperature measurements during LOFWOS#13: experimental measurements (red), CATHARE (green) and MATHYS (blue) predictions.

CATHARE and MATHYS predictions for the PIOTA2 and PIOTA6 measurements are presented on Figure 10. Both measurements present a short-term temperature peak during the initial power/flow decrease: then, temperatures decrease as the large negative reactivity insertion from the GEMs depresses core power, then rise again as the pumps finish coasting down. Temperatures hit a second peak as the flowrate reaches its natural convection state, then slowly decrease until the end of the transient. We observe that:

- CATHARE and MATHYS predict the timing of the first, short-term peak in both S/As, but tend to underestimate it to different extents;
- CATHARE predicts a second, natural-convection peak that is both later and higher than observed experimentally, dramatically so in the case of PIOTA6. Conversely, MATHYS predicts the PIOTA2 temperature peak quite well, and is also able to predict the low level of the second peak in PIOTA6.

Figure 11 provides more detail on the temperature fields calculated by TrioMC in the MATHYS simulation. In the fissile core, TrioMC predicts a radial temperature gradient in each S/A, as is commonly encountered in SFR subassemblies: this gradient reduces progressively as the sodium moves upwards, but is still close to 20°C in PIOTA2 and 12°C in PIOTA6 at the measurement level. Hence, the exact temperature level measured at PIOTA2 and PIOTA6 is strongly affected by the radial position of the probe, and can only differ from the average temperature predicted by CATHARE.

During the transient, several phenomena can affect the dynamics of the S/A outlet jet:

- during the transition to natural convection, the central, hotter part of the jet rises faster than its periphery, leading to a faster propagation of the second temperature peak from the core to the PIOTA2 probe. This effect probably explains why the second PIOTA2 peak occurs earlier in the experimental data and in MATHYS than in CATHARE. In the latter, the radial averaging of the temperature field behaves as a “cold plug” : this plug can only be evacuated by increased buoyancy in the sodium below. As a consequence, the PIOTA2 second temperature peak is also overpredicted by CATHARE.
- In the peripheral, PIOTA6 subassembly, the TrioMC temperature field at $t = 150$s (fig. 11, right) also shows strong radial cooling by the neighbouring cold reflector subassemblies through the inter-wrapper region: this even deviates the PIOTA6 outlet jet. This strong radial cooling explains why, in the MATHYS calculation, the second temperature peak is rather “flat” and limited, as in the ex-

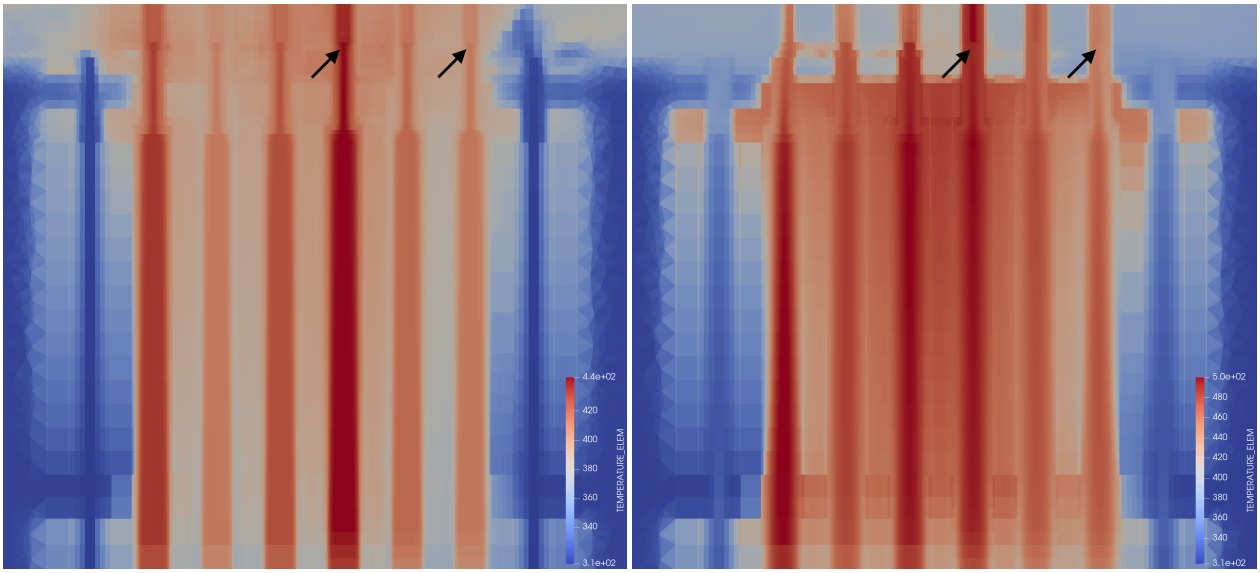

Figure 11. Vertical slice in the PIOTA2-PIOTA6 plane of in-core temperatures in the MATHYS simulation, from the top of the fissile core to the core outlet, at $t = 0$s (left) and at $t = 150$s (right). The PIOTA thermocouple locations are indicated by black arrows.

periment: the higher temperatures reached inside the PIOTA6 S/A never reach the core outlet level. On the contrary, the CATHARE calculation is unable to predict this effect: it also suffers from the "cold plug" effect caused by radial averaging described above, leading to the late and especially high temperature peak visible in Figure 10 (right).

The MATHYS predictions for PIOTA2 and PIOTA6 could still be improved: it seems, for instance, that an overestimation of the thermal inertia in the top of the subassemblies may explain the current underprediction of the initial temperature peak in both S/As. The TrioMC simulation at the core outlet is probably too coarse to correctly capture the jet dynamics from the top of the bundle to the PIOTA probes: a detailed CFD in this region would probably uncover more complex behavior. For instance, the temperature fluctuations present in the PIOTA6 experimental data are probably caused by turbulent jet oscillations: these could only be simulated by a LES or DNS CFD simulation. Finally, TrioMC seems to somewhat underestimate the radial heat transfers affecting PIOTA6.

As the above shows, the local measurements provided by the PIOTA are hard to relate to their CATHARE predictions. Discrepancies are caused by the radial temperature gradient in each S/A, which generates deviations between the average value computed by CATHARE and the local measurement point; however, additional discrepancies are caused by more "guenuine" 3D effects, such as radial heat transfers through the inter-wrapper region. In both cases, the availability of a finer simulation, such as the MATHYS simulation in this article, can provide insights into the experimental behavior.

CONCLUSION

Two simulations of the FFTF LOFWOS#13 test at imposed experimental power were performed in order to assess the impact of local thermal-hydraulic effects on this reactor transient: a CATHARE system-scale simulation and a MATHYS multi-scale simulation coupling the CATHARE model to a TrioMC/TrioCFD

model of the primary vessel.

Among the local phenomena simulated by MATHYS, only the onset of stratification in the upper plenum of the primary pool had an effect on the overall parameters of the transient, resulting in a stagnant temperature trend in the primary hot legs (figure 6, left). However, this effect is then dampened by the transient boundary conditions, in which the secondary loops are kept in forced convection: as a consequence, all other parameters are similar in the CATHARE and MATHYS simulations, and can already be well-predicted at the system scale.

This situation reverses when considering the two local core outlet temperature measurements provided in the LOFWOS#13 benchmark: these measurements are affected by a number of local effects that can only be predicted and understood by the more complex MATHYS simulation. A radial temperature gradient at the S/A outlets makes it hard to relate the local temperature measured experimentally to the average computed at the system scale, while radial heat transfers through the inter-wrapper region can, depending on the neighbourhood of each subassembly, decorrelate the temperature observed at the core outlet from the maximum temperature reached below. in both cases, the availability of a fine simulation can serve as a "numerical twin" to the experiment, helping to reconstruct measurements that can be compared more easily to the STH scale.

This situation is caused in part by the loop-type design of FFTF, which limits the impact of 3D effects, but also by the chosen transient boundary conditions, in which forced convection in the secondary loops acts as a strong "imposed-temperature" IHX. This second effect was also encountered in the PHENIX end-of-life natural convection test [1]: in that test as well, global transient parameters could be predicted very well at the system scales, while finer simulations were mainly useful to explain local phenomena, such as the behavior of IHX outlet jets. Two conclusions can be drawn from this exercice on the role of multi-scale simulations:

- even in cases where they are not necessary to predict the global behavior of a reactor transient, finer simulations may be used, as a "numerical twin", to better understand the impact of 3D phenomena on local measurements. If these local phenomena have no global impact, then it may not be necessary to couple these simulations to the global STH model: instead, they may be run in a second step, as a sort of post-processing.
- integral validation on reactor transients in which 3D effects have little-to-no global consequences may be insufficient if, in the targeted reactor design, these 3D effects are expected to play a larger role. For instance, in the French ASTRID design, around 30% of the decay heat can be removed by inter-wrapper flow in natural convection: the validation of such a prediction can not rely solely on integral transients in which the inter-wrapper flow plays a much smaller role. In such a situation, IETs or additional reactor transients would be necessary to provide additional validation coverage.

References

1. D. PIALLA et al., "Overview of the system alone and system/CFD coupled calculations of the PHENIX Natural Circulation Test within the THINS project," *Nuclear Engineering and Design*, **290**, *Supplement C*, 78 (2015).
2. H. UITSLAG-DOOLARD et al., "Multiscale modelling of the PHENIX dissymmetric test benchmark," SESAME International Workshop, 2019.
3. *Benchmark Analysis of EBR-II Shutdown Heat Removal Tests*, IAEA, Vienna (2017).
4. "Benchmark Analysis of FFTF Loss Of Flow Without Scram Test," 2018.

5. A. GERSCHENFELD, "Towards more efficient implementations of multiscale thermal-hydraulics," *Nuclear Engineering and Design*, **381**, 111322 (2021).
6. C. D. FLETCHER and R. R. SCHULTZ, "RELAP5/MOD3 Code Manual,".
7. D. TENCHINE et al., "Status of CATHARE code for sodium cooled fast reactors," *Nuc. Eng. and Des.*, **245**, 140–152 (2012).
8. U. NRC, "Trace v5. 0 theory manual, field equations, solution methods, and physical models," *United States Nucl. Regul. Comm* (2010).
9. C. TZANOS, "Decay heat removal by natural convection-the RVACS system.," Argonne National Lab., IL (US) (1999).
10. T. EZURE, J. KOBAYASHI, T. ONOJIMA, A. KURIHARA, and M. TANAKA, "PLANDTL-2 Experiment for Evaluation of Decay Heat Removal in Sodium-cooled Fast Reactors," AESJ 2018 Fall meeting, 2018.
11. V. NARCISI, F. GIANNETTI, M. POLIDORI, M. TARANTINO, and G. CARUSO, "RELAP5-3D© AND MODIFIED RELAP5 CALCULATION COMPARISON FOR A PLOHS + LOF TRANSIENT IN CIRCE-ICE TEST FACILITY," 09, 2019.
12. A. CONTI, A. GERSCHENFELD, and R. LAVASTRE, "Numerical analysis of core thermal-hydraulic for sodium-cooled fast reactors," NURETH-16, 2015.
13. P.-E. ANGELI, U. BIEDER, and G. FAUCHET, "Overview of the TrioCFD code: Main features, VetV procedures and typical applications to nuclear engineering," *Proc. NURETH 16 - 16th International Topical Meeting on Nuclear Reactor Thermalhydraulics*, 2015.
14. J. PACIO et al., "Inter-wrapper flow: LBE experiments and simulations," NURETH18, 2019.
15. D. GRISHCHENKO et al., "The TALL-3D facility design and commissioning tests for validation of coupled STH and CFD codes," *Nuc. Eng. Des.*, **290**, 144 (2015).
16. H. KAMIDE et al., "Investigation of Core Thermohydraulics in Fast Reactors—Interwrapper Flow during Natural Circulation," *Nuclear Technology*, **133**, *1*, 77 (2001).
17. D. M. LUCOFF, "Passive Safety Testing at the Fast Flux Test Facility," *Nuclear Technology*, **88**, *1*, 21 (1989).
18. J. B. WALDO, A. PADILLA JR, D. NGUYEN, and S. CLAYBROOK, "Application of the GEM Shutdown Device to the FFTF Reactor," *Trans. Am. Nucl. Soc.;(United States)*, **53**, *CONF-861102-* (1986).
19. C. CABELL, "Summary Description of the Fast Flux Test Facility," Hanford Engineering Development Lab., Richland, WA (USA) (1980).
20. K. REHME, "Pressure drop correlations for fuel element spacers," *Nuclear technology*, **17**, *1*, 15 (1973).
21. E. SKUPINSKI, J. TORTEL, and L. VAUTREY, "Determination des coefficients de convection d'un alliage sodium-potassium dans un tube circulaire," *International Journal of Heat and Mass Transfer*, **8**, *6*, 937 (1965).
22. V. BORISHANSKII and E. FIRSOVA, "Heat transfer in separated rod bundles in a longitudinal flow of metallic sodium," *Journal of Nuclear Energy. Parts A/B. Reactor Science and Technology*, **19**, *2*, 143 (1965).
23. J. PACIO, S. CHEN, Y. CHEN, and N. TODREAS, "Analysis of pressure losses and flow distribution in wire-wrapped hexagonal rod bundles for licensing. Part I: The Pacio-Chen-Todreas Detailed model (PCTD)," *Nuclear Engineering and Design*, **388**, 111607 (2022).
24. S.-K. CHEN and N. TODREAS, "Hydrodynamic models and correlations for bare and wire-wrapped hexagonal rod bundles — Bundle friction factors, subchannel friction factors and mixing parameters," *Nuclear Engineering and Design - NUCL ENG DES*, **92**, 227 (1986).
25. A. Y. GUNTER and W. A. SHAW, "A general correlation of friction factors for various types of surfaces in cross flow," *Trans. ASME*, **67**, 643 (1945).
26. R. SEBAN and T. SHIMAZAKI, "Heat Transfer to a Fluid Flowing Turbulently in a Smooth Tube with Walls at Constant Temperature," *Trans. ASME*, **73** (1949).
27. A. GERSCHENFELD, Y. GORSSE, and G. FAUCHET, "Development of a Polyhedral Staggered Mesh Scheme: Application to Subchannel and CFD SFR Thermal-Hydraulics," NURETH-18, 2019.